Optical profiling on lateral spreading of space-charge-region metal-semiconductor-metal structures

S.Khunkhao [a] A.Thaworn [a] S.Somdetsakun [a] S.Nuanloy [a] S.Korchareon [b], S. Niemcharoen [b]

Department of Electrical engineering, Faculty of Engineering, Sripatum University, 61 Phahonyothin Road, Saenanikhom, Jatujak, Bangkok 10900, Thailand.Email: Sanya@spu.ac.th

[b] Electronics Research Center, Faculty of Engineering, King Mongkut's Institute of Technology Ladkrabang, Charongkrung Road, Ladkrabang, Bangkok, 10520 Thailand.Email: knsurasa@kmitl.ac.th

***Abstract*-Optical profiling on lateral spreading of space-charge-region properties of Schottky-barrier metal-semiconductor-metal (MSM) structures have been investigated experimentally. Making use of a planar molybdenum/n-type silicon /molybdenum (Mo/n-Si/Mo) MSM structure with a wide electrode separation, one-dimensional (1D) profiling of optical–beam intensity distribution from a helium-neon (He-Ne) laser was carried out. It was also confirmed that, in addition to existing photosensing function, the sensitivity (output photocurrent) of such a structure could be controlled by an applying bias via lateral spreading of the surface space-charge-region (SCR) at the side of the Schottky-junction reverse-biased.**

I. INTRODUCTION

The blocking (Schottky-barrier) metal-semiconductor-metal (MSM) structure is a viable and fundamental device structure in the field of light-wave communication and optical data processing systems. This structure provides several advantages such as wide-band operation, low-noise behaviour [1], ease of integration with other functions on the same chip and so forth [2].

Recently we experimentally confirmed that a planar MSM structure having a wide separation between the two metal electrodes exhibits not only the function of a basic optical sensor but also optical sensitivity field-controllable by the bias applied between the electrodes [4]. In this study, we present the experimental results of one-dimensional (1D) optical-beam profiling properties of an MSM structure as its application[2,3]. To our knowledge, no study has appeared on such an application of planar MSM structures.

II. MODEL OF OPERATION

The essential cross-section of the structure we treat in this study is illustrated schematically in Fig.1. The structure is of single-slit type (not interdigitated), the bird's eye view of which is also inset in Fig.1. Schottky-barrier is formed at each boundary between the metal and the semiconductor. The separation between the electrodes located at both ends is wide enough to leave the undepleted neutral region under the bias we examined. When a bias voltage is applied between the electrodes, one Schottky-junction is reverse-biased and the other junction is forward-biased.

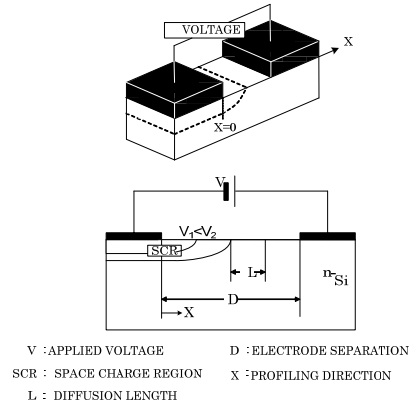

Figure 1. Schematic illustration of an MSM structure, leaving an undepleted region even under a bias.

Such a structure is expected to show lateral spreading of its space-charge-region (SCR) at the Schottky-barrier reverse-biased, the spreading of which is possible to be controlled by bias. According to the simplified model of such a structure, the width of the lateral spreading of the SCR of the Schottky-junction reverse-biased in the direction of profiling is expressed semi-empirically as[4]

$$W(V_a) = \sqrt{\beta(V_0 + V_a)} \qquad (1)$$

where $W(V_a)$ is the width of lateral spreading of the SCR along the surface of the active area at an applied bias V_a, $\beta = 2\varepsilon_s / qN_D$, ε_S is the permittivity of the semiconductor employed, q is the elementary charge, N_D is the impurity concentration and V_0 is the built-in voltage of the Schottky-barrier, respectively. The barrier on the other side is forward-biased and assumed to be nearly flattened for simplicity, although the residual undepleted region might exhibit an appreciable resistance reflecting its wide length. Therefore, when the influence of this resistance is taken into account, the applied bias V_a might be replaced by V_a-IR in (1), where I is the device average current and R is the equivalent series resistance. Thus, the photoinduced current $I_P(V_a)$ is approximately formulated as [4]:

$$I_p(V_a) = \eta[kW(V_a) + L] \qquad (2)$$

where L is the diffusion length of the semiconductor and k means that the SCR is k-times more effective to generate the photocurrent than the residual undepleted region (presumably, larger than unity, and η is the proportionality factor including the effect of quantum efficiency and intensity level of irradiation. As a result, $I_P(V_a)$ is would be an increasing function of applying bias V_a with the dependence on $\sqrt{V_0 + V_a}$ This means that the device structure under consideration is to furnish the field-controllable iris, although the equivalent size as a pixel also increases in the direction of profiling with the bias applied.

III. EXPERIMENTAL

A. Sample description

To make the electrodes of $3\times3\ \mathrm{mm}^2$, molybdenum film working also as barrier metal was deposited onto an n-type silicon wafer by an electron-beam evaporator and was subsequently processed by photolithography lift-off technique. The electrode separation is mainly 2000 μm. The resistivity of the wafer used was $(40\text{-}50)\,\Omega\mathrm{cm}$. This resistivity would provide corresponding donor concentration of some $3\times10^{16}\mathrm{cm}^{-3}$. The height of the Schottky-barrier on both sides was estimated to be $(0.55\text{-}0.65)\,eV$ from the forward current–voltage characteristic[5]. Furthermore, from this value of the barrier-height, the built-in voltage V_0 is deduced to be approximately $0.23\,eV$

B. Optical profiling procedure

Here we examine profiling of the light-beam from a He-Ne laser, the wave length of which is 633nm. The experimental system for profiling was arranged to suppress the influence of the stray light including reflected light from the ambient surfaces of the sample under test. The orientation of the incident light from the light source was tilted a little from the normal line of the active area of the device in the plane perpendicular to the profiling direction. The optical beam was scanned by every 15 μm in the perpendicular orientation of the tilting plane of the beam. Correspondingly, the influence of the tilt of the beam is presumably minimized in 1D direction where we are intending to profile. Spatial intensity distribution of the beam to be detected was assumed to be Gaussian distribution with the radius (2σ) of 480 μm defined at the point of $1/e^2$ its maximum just at the aperture of the light source quoted by the manufacturer [6]. The dispersion angle of the beam from the source is approximately $0.23\,mrad$. To control the light intensity incident onto the sample, a neutral density (ND) filter was utilized. Furthermore, since the electrode separation is wide, no interference of incident light is assumed at the very edge of each electrode.

IV. RESULT AND DISCUSSION

A. 1D-profiling properties

We observed the spatial distribution of detected photocurrent over the whole region between the electrodes, the typical plot of which is shown in Fig. 2.

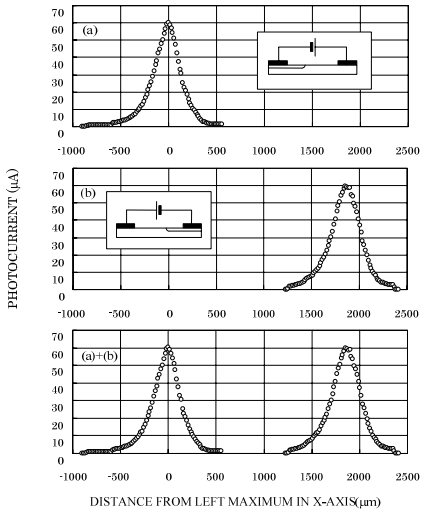

Figure. 2. Spatial distribution of the photocurrent under a constant optical illumination level versus the lateral position of every 15 μm step. Electrode separation is 2000 μm.

The photocurrent was obtained by subtracting the dark current from the current as measured at the same bias. Each peak in the Fig.2(a) and (b) corresponds to the profile when the polarity of applied bias is reversed. From the Fig. (a)+(b), the separation of the two peaks is estimated to be about 1920 μm, which is a little smaller than the electrode separation.

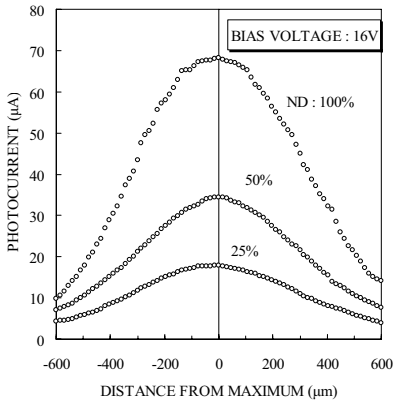

Figure.3. Photocurrent distribution under three different intensities of illumination at $V_a = 16\mathrm{V}$ for the same sample appeared in Fig.2.

It is apparent from these Figures that only the SCR of the junction reverse-biased generates significant photocurrent. On the contrary, the current from the barrier forward-biased on the other side is extremely small and is substantially ignored. Therefore, these two similar peaks must correspond to the photocurrent dominantly from the SCR of respective junction reverse-biased, showing k is larger than unity. Therefore, these results suggest that the region where no detectable photocurrent is observed can be treated to have substantially flat band.

Figure 3 shows the photocurrent versus position relationship for the sample appeared in Fig. 2 under a bias of 16V at the distance of 10cm from the aperture of the light source, taking the intensity of the illumination as a parameter. Here the light intensity was controlled by an ND filter between 25 per cent and 100 per cent of its maximum. One finds that the level of each peak corresponds to the optical intensity level.

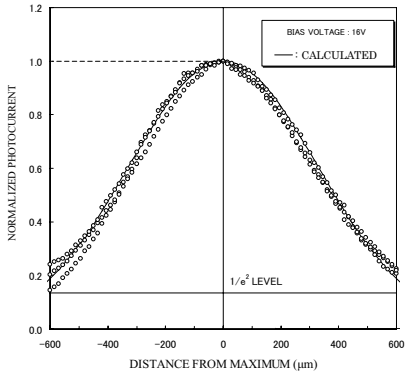

Figure.4. Normalized plot of the spatial current distribution from the data in Fig.3. Solid line represents the calculated Gaussian distribution for reference, taking $2\sigma = 480\mu m$.

Furthermore, the normalized plots from the data in Fig.3 are shown in Fig.4, where the solid line represents the Gaussian curve calculated from the parameters given by the manufacturer of the light source. A good agreement has been obtained between the experimental plots for different illumination levels and the plot theoretically expected. We also performed the profiling at the several different distances from the light source ranging from 10cm to 60cm. The plots given in Fig. 5 are the ones showing the detected current distribution of the beam versus the distance from each maximum.

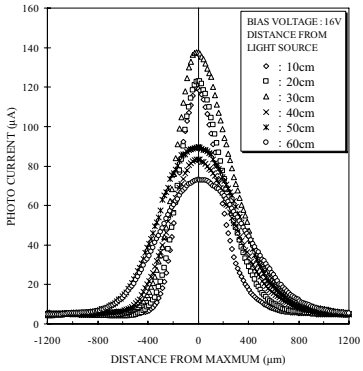

Figure.5. 2σ dependence of the spatial distribution of current on the distance from the light source.

From the data in Fig. 5, halves of normalized curves are replotted in Fig. 6, where the solid lines correspond to the lines calculated respectively. It is found that a good agreement has also been achieved between the experimental and calculated plots. In Fig. 7 is shown the radii of the optical beam experimentally obtained and numerically expected with respect to the distance from the light source for the case $V_a = 16V$. With increasing the distance, the difference between these two plots seems to decrease.

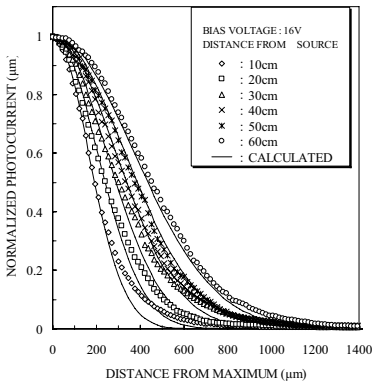

Figure.6. Normalized profiles of currents with respect to the distance from the maximum, where solid lines were calculated, respectively.

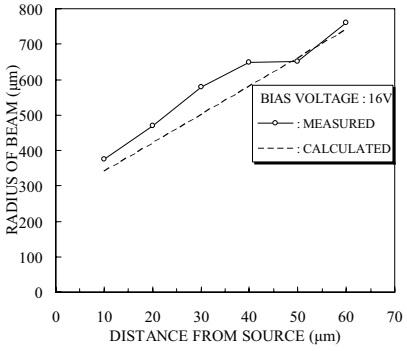

Figure.7. Experimental and calculated radii of the beam versus distance from light source.

This is curious a little. Generally, an increase in the difference between the two plots is expected with increasing the distance from the source.

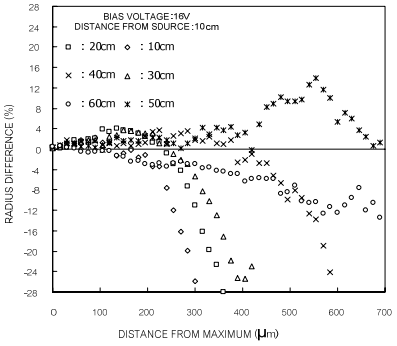

Figure. 8. Dependence of the difference in radii between experimentally observed and calculated on distance from the maximum.

In order to clarify this result further, we plotted in Fig. 8 the dependence of the difference in per cent between the experimental and calculated plots on the distance from the intensity maximum point, where the distance from the source was taken as a parameter. On the contrary, the difference seems to increase more or less with the distance from its maximum. These results observed might be attributed to incompleteness of avoiding the influence of stray light on the measured photocurrents. That is, with increase in the distance from the source, the influence of stray light on the profiling decreases.

B. Field-controllability of profiling

We also carried out profiling by changing the bias voltage. Fig. 9 pictures the experimental plots for V_a=2V, 4V and 16V biases. In Fig.10, the plots normalized at the peak value are shown, where the solid line corresponds the level theoretically expected. Again, a good agreement has been obtained from the view point of the level predicted, while the beam size being substantially unchanged even under the change in the bias applied. As a result, it can be concluded that the planar MSM structure examined can be used as a simple intensity profiler of an optical-beam of this size.

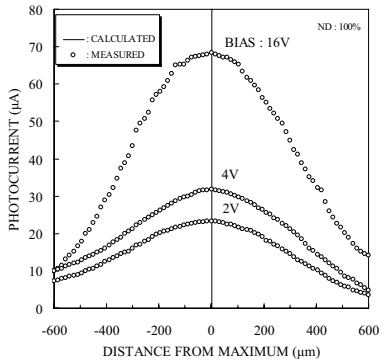

Figure.9. Bias dependence of experimental spatial intensity distribution for $Va = 2V, 4V$ and 16V.

However, it should be in mind that the detected spatial distribution of the current is for the photocurrent essentially given by (2). Therefore, with the increase in bias, the width of the SCR also increases following (1), which means the increase in size of the pixel. We used, in the present experiments, the silicon wafer of the resistivity of (40-50)Ωcm for preparing samples. This resistivity expects the change in the width of the SCR, $W(V_a)$, from 6 μm to 16 μm at most between 2V and 16V. As mentioned earlier, the profiling was carried out changing the relative position by every 15 μm step, which is still larger or approximately equal comparing to the width of the SCR.

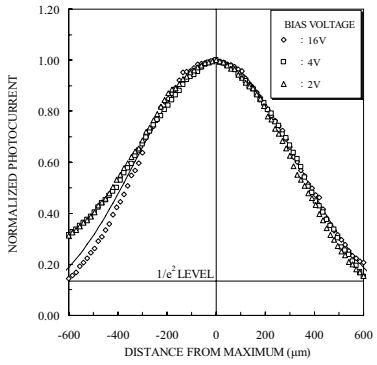

Figure. 10. Profiling normalized at the maximum for the bias V_a=2V,4V and 16V obtained from Fig.9.

Therefore, it can be mentioned that the beam profiling would still be effective. We repeated the similar measurements on the structure having 20 μm electrode separation. In spite that the diffusion length estimated to be 70 μm must be considered in generating photocurrents, no direct evidence of the contribution from the diffusion current was observed. This result might be attributed that the SCR is several times more efficient than the same area within the diffusion length in generating photocurrent [4,5]. Therefore, one can mention that the structure examined in this study is usable as a pixel for 1D optical-beam profiling, having the field-controllable sensitivity. It can also be mentioned that the increase in detected photocurrent is explained by the reflection of the photoexcited current due to the carriers laterally accumulated by spreading of the SCR with an applied bias. It is of interest that the effect of an optical spot position on the performance of MSM structures with no applied bias has been investigated previously [5]. This method, however, utilizes solely the current generation via photoexcitation of carriers like a solar cell. Therefore, the operation mechanism of this structure is essentially different from that of the structure we proposed in the present study.

V. CONCLUSION

As a novel application, a planar MSM (metal-semiconductor-metal) structure has been applied to profiling of the spatial intensity distribution of an optical beam in visible range. The Gaussian intensity distribution of the beam from a He-Ne laser was confirmed experimentally. The MSM structure proposed in this study also exhibits field-controllable sensitivity making use of lateral spreading of the SCR (space-charge-region) at the active surface. The performance of this structure is well explained by the simplified model.

ACKNOWLEDGEMENT

The authors wish to thank Prof.Dr.Kazunori Sato, Assoc.Dr.W. Titiroongruang and S.Niemcharoen of King Mongkut's Institute of Technology for valuable discussions and comments throughout this work. Continuous encouragement of Dr.R.P.Phukkamarn of Sripatum University is deeply appreciated. This work was supported in part by The Thailand Research Fund and Commission on Higher Education (Grant No.MRG5080004)

REFERENCES

[1] Burroughes JH., Rogers DL., Arjavalingam G., Pettit GD.,and Goorsky MS.,1991,*Doping induced bandwidth enhancement in metal-semiconductor-metal photodetectors*,IEEE Photonics Letters;3,657-659

[2] Safwat AME., Lin CK., Kim J., Johnson FG., Johnson WB., Goldsman N., Lee C., 2000, *Investigation of the optical spot position on the performance of metal-semiconductor-metal structures: novel application*. Solid-State Electronics, 44, 2077-2080.

[3] Yuang RH., Shieh JL., Chyi JI., and Chen JS., 1997, *Overall performance improvement in GaAs MSM photodetectors by using recessed-cathode structure*, IEEE Photonics Letters, 9, 226-228

[4] Khunkhao S., Yasumura Y., Kitagawa K., Masui T., and Sato K., 2003, *On laterally spreading of space-charge-region in planar metal-semiconductor-metal structures*. Solid-State Electronics., 47, 1811-1816.

[5] Masui T., Khunkhao S., Kobayashi K., Niemcharoen S., Supadech S., and Sato K., 2003, *Photosensing properties of interdigitated metal-semiconductor-metal structures with undepleted region*, Solid-State Electronics, 47, 1385-1390.

[6] Arafa M., Wohlmuth WA., Fay P., and Adesida I., 1998, *Effect of Diffraction and Interference in Submicron Metal-Semiconductor-Metal Photodetectors*, IEEE Transactions on Electron Devices, ED-45, 62-67.